

Abstract

The study of the emission properties of supernova remnants (SNRs) gives us relevant information about their morphology, properties of the ejecta, and shock fronts, with which it is possible to reconstruct the progenitor's past evolution history. In this work, we have focused on one of the most studied SNRs due to its morphology: Kepler's SNR.

We have studied this remnant's non-thermal emission in both radio and X-rays using synthetic emission maps generated through 3D MHD numerical simulations. We propose that non-thermal X-ray emission is due to the Inverse Compton (IC) mechanism, while radio emission is generated by synchrotron radiation.

Our simulations: "ears" formation

Kepler's SNR is a young remnant, approximately 420 years old [7]. The distance to the SNR is between 4.8 and 8.2 kpc [6].

In our work, we propose the following scenario to explain the "ears" type morphology of Kepler's SNR:

A runaway AGB progenitor star creates a double shock wind structure [1], thus modifying the conditions of the circumstellar medium. In this structure, a type Ia SN explosion is generated with an asymmetry, the result of launching two conical jets just at the moment of the explosion, [1, 8, 3]

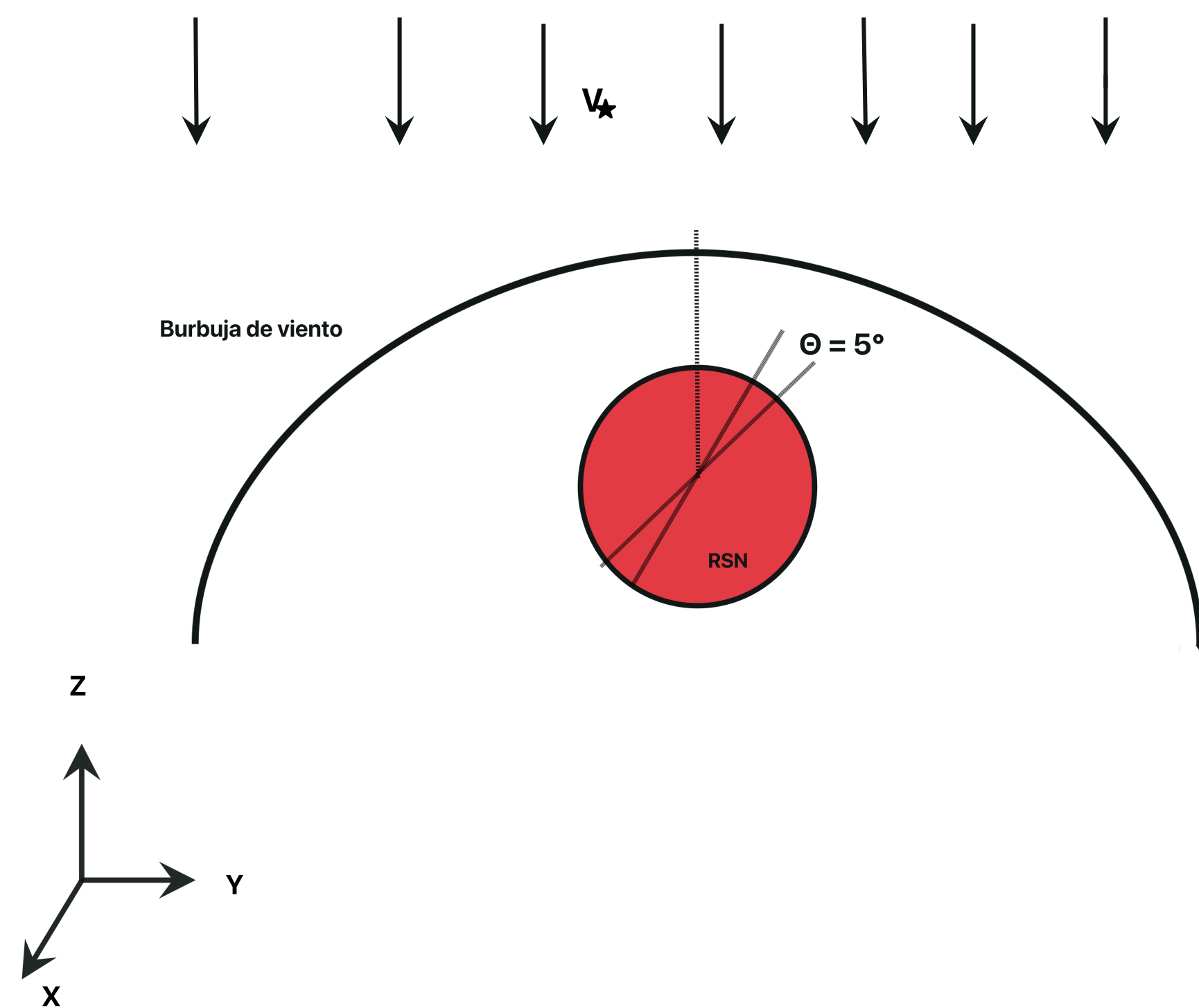


Figure 1. Initial features of the scenario: AGB wind + SNR + Jets. The opening angle of the jets is 5°, forming an angle of -70° respect to the Z axis.

The code: The initial setup

We use the GUACHO numerical code to make 3D magnetohydrodynamic numerical simulations of this scenario to compute synthetic maps of non-thermal emission in X-rays (through the IC mechanism) as well as in radio, [5].

Our computational domain consists of a $12 \times 12 \times 12$ pc box and 32 processing cores with a resolution of $512 \times 512 \times 512$ pixels.

| ISM | AGB Wind | Jets + SN |
|--|--|-----------------------------|
| $n_0 = 1 \times 10^{-3} \text{ cm}^{-3}$ | $\dot{M} = 1.5 \times 10^{-5} M_{\odot} \text{ yr}^{-1}$ | $M_0 = 2.11 M_{\odot}$ |
| $ B_{ISM} = 2 \mu\text{G}$ | $R_w = 0.46 \text{ pc}$ | $E_0 = 10^{51} \text{ erg}$ |
| $V_{ISM} = 280 \text{ km/s} = V_*$ | $V_w = 10 \text{ km/s}$ | $V_{jet} = 5V_0$ |
| $T_{ISM} = 5000 \text{ K}$ | $\tau = 300 \text{ kyrts}$ | $\tau = 500 \text{ yrs}$ |

Table 1. Parameters used in the simulation for both the Interstellar Medium (ISM), the AGB wind and the SN explosion

Why do we propose the Inverse Compton process?

In both radio and X-rays, Kepler's SNR is observed as an incomplete shell, brighter towards the northwest [2]. Non-thermal X-ray emission has also been observed in this object [11], which could be thought to have the same origin as in the radio (by the synchrotron mechanism). However, the morphology doesn't coincide with the synchrotron emission in radio, so we propose another type of non-thermal emission in X-rays: emission due to the IC process.

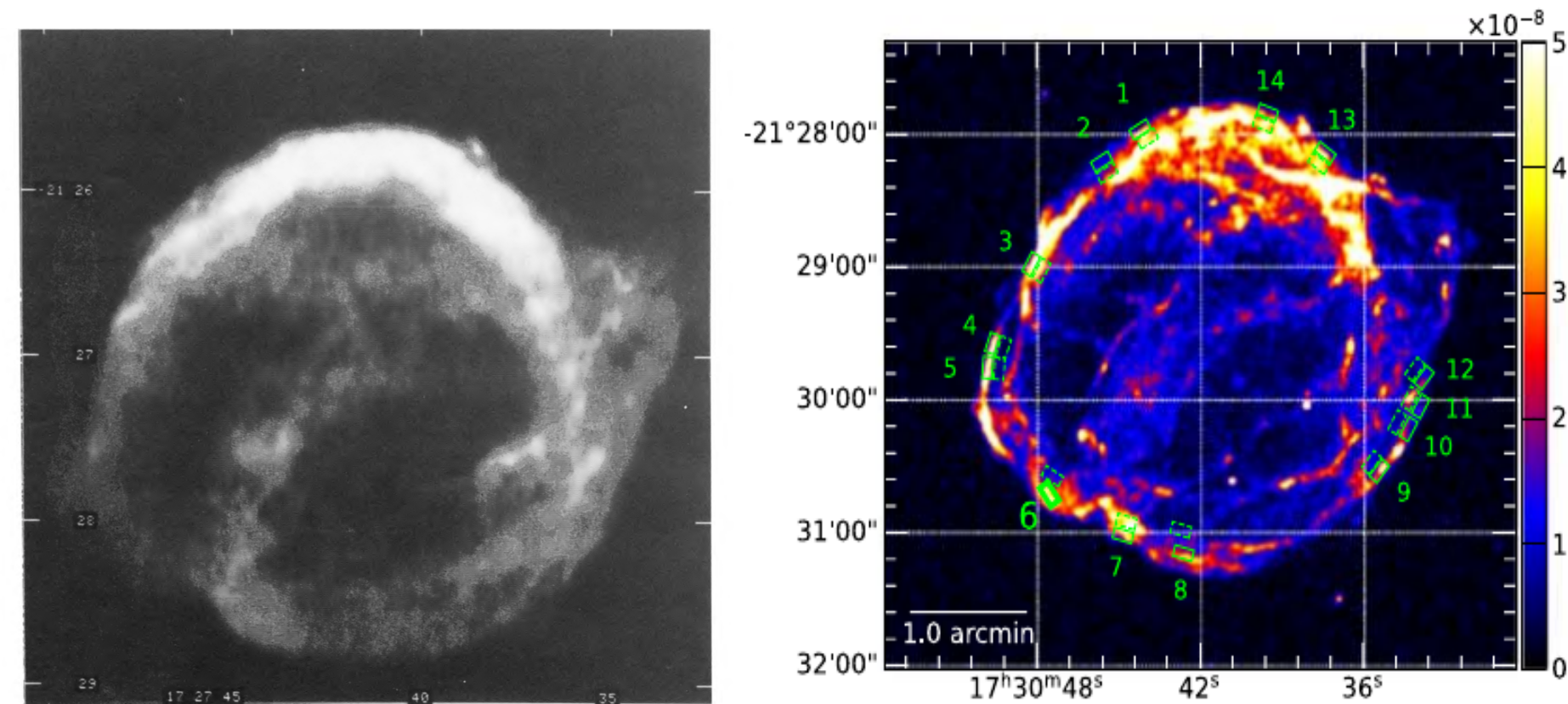


Figure 2. Left map: radio observations made by the VLA [4], right map: X-ray flow images in the range of [4-6] keV, taken by Chandra [11].

Non-thermal X-rays: Inverse Compton

We have low energy photons interacting with relativistic electrons. Following the idea of Villagran et al. (2024) [12], the electrons that caused the synchrotron emission are the ones that could start the IC process. Radiative cooling (Q_L) was considered as the main source of photons for the IC mechanism.

Results: Comparing with the observations

Runaway star AGB wind + Asymmetric SN with jets = EARS!

Once considering the conditions of Table 1 and the scenario of our simulation, it is possible to obtain the density maps which are slices of the data cube. The simulated Kepler's SNR was allowed to evolve 450 years after imposing the initial condition of the explosion within the region modified by the AGB wind; see Figure 3.

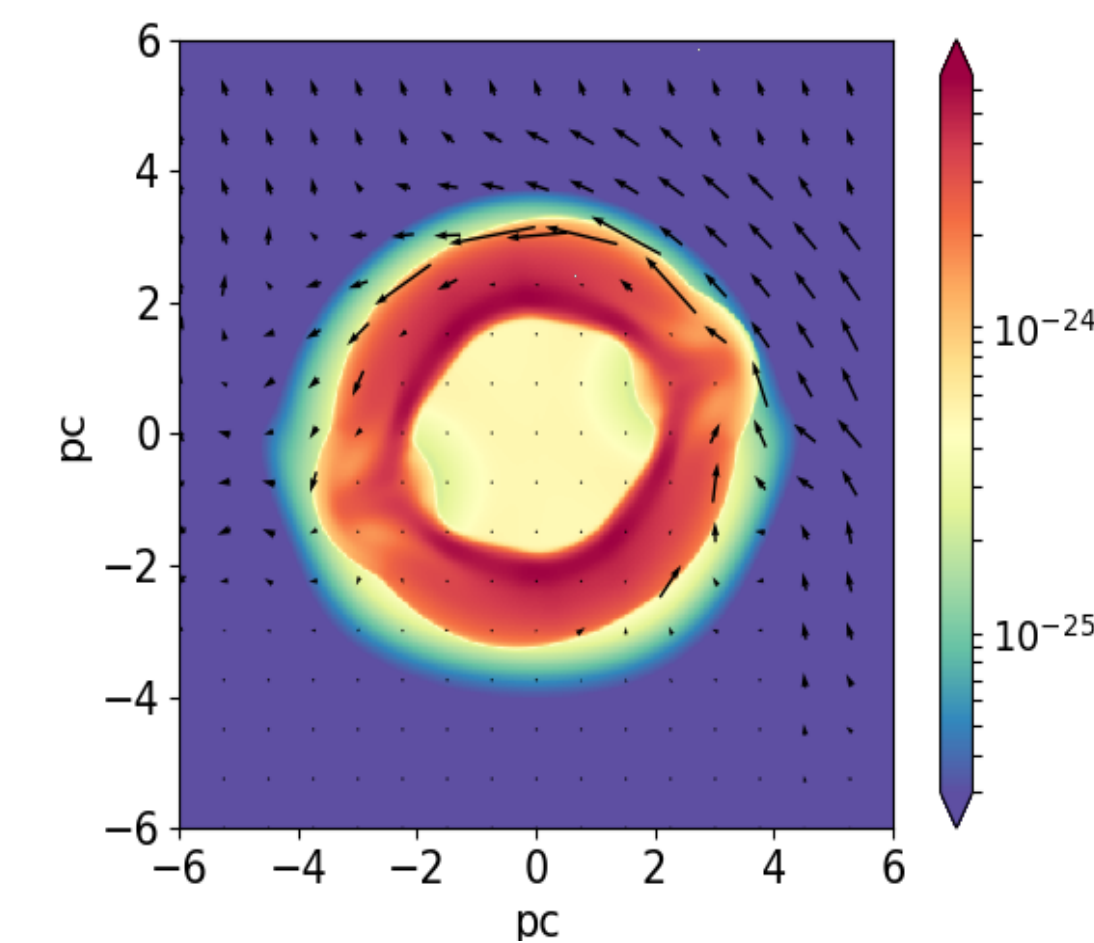


Figure 3. Mass density cut in the YZ plane at $x = 6$ pc corresponding to a simulation time of 450 years, considering an initial remnant of approx. 35 years.

In Figure 4 we can see that the brightness distribution of the synchrotron emission map obtained with our results coincides with the emission map of the observations made by VLA.

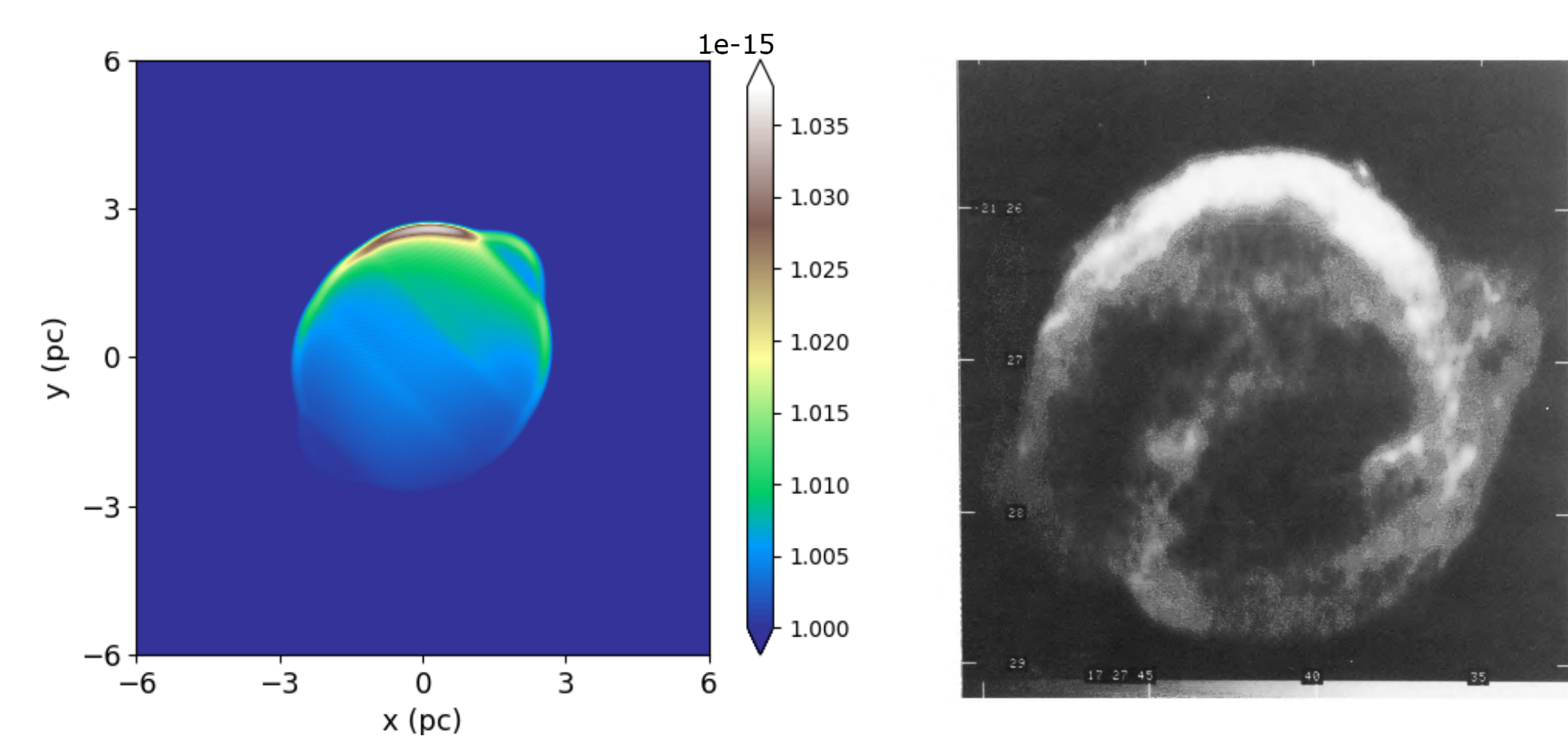


Figure 4. Comparison of the radio emission map obtained with the numerical simulation data (left side) given in $\text{erg s}^{-1} \text{ cm}^{-2} \text{ sr}^{-1}$, and the emission map of the observations made by the VLA [4].

Figure 5 shows the non-thermal X-ray emission maps considering the IC process with two different energy densities: radiation produced by Q_L and radiation from H_{α} emission, the emission being greater considering Q_L (left side).

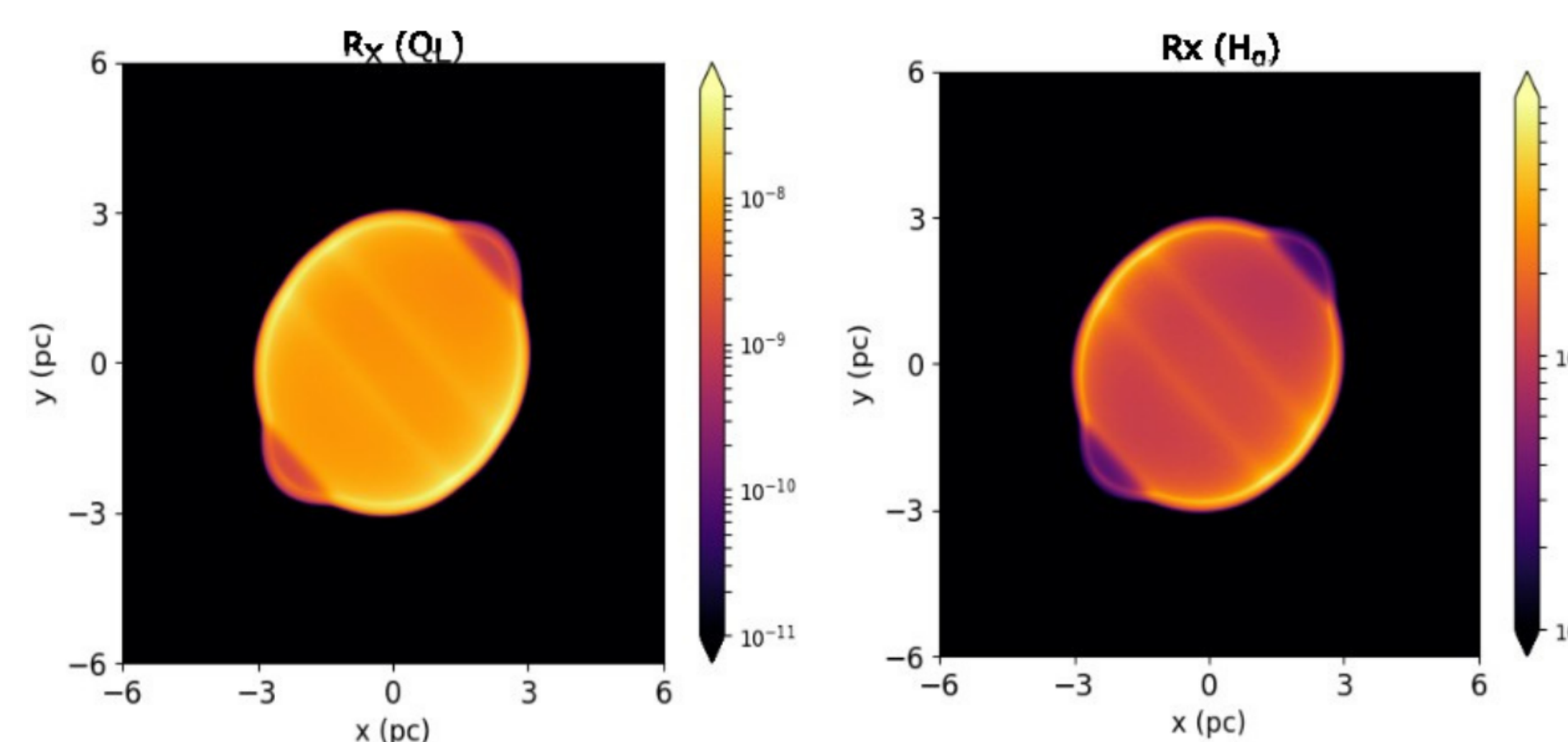


Figure 5. Non-thermal X-ray emission map considering the IC emission process given in $\text{erg s}^{-1} \text{ cm}^{-2} \text{ sr}^{-1}$ in an energy range of 2-4 keV. Left side: emission map considering a radiation background from the QL radiative cooling. Right side: IC emission resulting from H_{α} .

Conclusions

- ★ An asymmetrical explosion seems to be the best scenario for obtaining "ears". This asymmetry is due to differences in the ejecta speed distribution related to jets.
- ★ Our model generally reproduces Kepler's SNR's "ears" type morphology.
- ★ We suggest that the brightness distribution observed in non-thermal X-ray results from the emission produced by IC. Two radiation sources are considered: radiative cooling (Q_L) and the emission of H_{α} , radiative cooling being more efficient.
- ★ IC emission opens a new panorama in studying SNRs where radio and X-ray emissions don't match.

References

- [1] R. Bandiera. On the Origin of Kepler's Supernova Remnant. *The Astrophysical Journal*, 319:885, Aug. 1987.
- [2] W. P. Blair, P. Ghavamian, K. S. Long, B. J. Williams, K. J. Borkowski, S. P. Reynolds, and R. Sankrit. Spitzer space telescope observations of kepler's supernova remnant: A detailed look at the circumstellar dust component. *The Astrophysical Journal*, 662:998 – 1013, 2007.
- [3] Chiotellis, A., Schure, K. M., and Vink, J. The imprint of a symbiotic binary progenitor on the properties of kepler's supernova remnant. *A&A*, 537:A139, 2012.
- [4] J. R. Dickel, R. Sault, R. G. Arendt, Y. Matsui, and K. T. Korista. The Evolution of the Radio Emission from Kepler's Supernova Remnant. *A&A*, 330:254, July 1988.
- [5] Esquivel, A., Raga, A. C., Cantó, J., and Rodríguez-González, A. The interaction of an o star wind with a herbig-haro jet. *A&A*, 537:2855–860, 2009.
- [6] M. J. Millard, J. Bhalerao, S. Park, T. Sato, J. P. Hughes, P. Slane, D. Patnaude, D. Burrows, and C. Badenes. An Ejecta Kinematics Study of Kepler's Supernova Remnant with High-resolution Chandra HETG Spectroscopy. *The Astrophysical Journal*, 893(2):98, Apr. 2020.
- [7] S. P. Reynolds, K. J. Borkowski, U. Hwang, J. P. Hughes, C. Badenes, J. M. Laming, and J. M. Blondin. A deep chandra observation of kepler's supernova remnant: A type Ia event with circumstellar interaction. *The Astrophysical Journal*, 668(2):L135, oct 2007.
- [8] N. Soker, E. García-Berro, and L. G. Althaus. The explosion of supernova 2011fe in the frame of the core-degenerate scenario. *Monthly Notices of the Royal Astronomical Society: Letters*, 437(1):L66–L70, oct 2013.
- [9] J. C. Toledo-Roy, A. Esquivel, P. F. Velázquez, D. M. A. Meyer, and E. M. Reynoso. A 3D numerical model for Kepler's supernova remnant. *Monthly Notices of the Royal Astronomical Society*, 442(1):229–238, 06 2014.
- [10] D. Tsebrenko and N. Soker. ACCELERATING VERY FAST GAS IN THE SUPERNOVA IMPOSTOR SN 2009ip WITH JETS FROM A STELLAR COMPANION. *The Astrophysical Journal*, 777(2):L35, oct 2013.
- [11] N. Tsuji, Y. Uchiyama, D. Khangulyan, and F. Aharonian. Systematic Study of Acceleration Efficiency in Young Supernova Remnants with Nonthermal X-Ray Observations. *The Astrophysical Journal*, 907(2):117, Feb. 2021.
- [12] M. A. Villagran, D. O. Gómez, P. F. Velázquez, D. M. A. Meyer, A. Chiotellis, A. C. Raga, A. Esquivel, J. C. Toledo-Roy, K. M. Vargas-Rojas, and E. M. Schneller. Simulated non-thermal emission from SNR G1.9+0.3. [arXiv:2309.14410](https://arxiv.org/abs/2309.14410), Sept. 2023.